Biosensors and Bioelectronics 186 (2021) 113285

Contents lists available at ScienceDirect

Biosensors and Bioelectronics

journal homepage: www.elsevier.com/locate/bios

Short communication

Silicon carbide nanoparticles electrospun nanofibrous enzymatic glucose sensor

Kavyashree Puttananjegowda *, Arash Takshi, Sylvia Thomas

Department of Electrical Engineering, University of South Florida, Tampa, Florida, USA

ARTICLE INFO

Keywords:
Silicon carbide nanoparticles
Conductive polymer
Glucose oxidase enzyme
Electrospun nanofibrous membrane
Electrochemical
Biosensor

ABSTRACT

This paper presents an electrospun-nanofibrous-membrane (ENFM) of silicon carbide nanoparticles (SiCNPs) with a conductive polymer (CP) for an electrochemical enzymatic glucose sensor. The surface area of a fiber matrix is a key physical property of a nanofiber membrane for enzyme binding. It is found that glucose sensing electrodes, having a SiCNPs-ENFM nanostructure, show enhanced binding of glucose oxidase (GO_x) enzyme within the fibrous membrane. Morphological characterization of SiCNPs based ENFM was performed by using scanning electron microscopy (SEM) and using transmission electron microscopy (TEM) for SiC nanoparticles. The electrochemical analysis of SiCNPs-ENFM electrode was conducted by using cyclic voltammetry (CV), electrochemical impedance spectroscopy (EIS) and chronoamperometry (CA) methods. Glucose concentration was detected at +0.6 V in a 5 mM potassium ferricyanide electrolyte. SiCNPs-ENFM based glucose electrodes show a detection range from 0.5 mM to 20 mM concentration with the sensitivity of 30.75 μA/mM cm^2 and the detection limit was 0.56 μM. The lower change in current response for SiCNPs-ENFM based glucose sensing electrodes was observed for a 50 day period.

1. Introduction

In latest years, considerable progress has been made in the development of highly sensitive, highly durable, low-cost, point-of-care and accurate biosensors that can continuously monitor different health care issues such as glucose levels of a diabetic patient (Le et al., 2019; Puttananjegowda and Thomas, 2018, 2020). Glucose sensors are used to measure the glucose concentration of a blood in a patient and are an important part of managing diabetes mellitus (American Diabetes Association, 2020; Puttananjegowda and Thomas, 2017). However, a serious challenge for implantable devices is the durability of the sensing material being exposed to blood for a long period of time. Degradation of the sensing material limits the device longevity, sensitivity, and may cause other medical complications for the patient. Silicon carbide (SiC) is one of the biocompatible material, has been used in many biomedical devices (Koschwanez and Reichert, 2007; Gabriel et al., 2007; Saddow et al., 2010; Xu et al., 2019; Ababneh et. al., 2017). Clinical studies of SiC being used in bone prosthetics, heart stents, and implantable glucose sensors have confirmed the material's biocompatibility (Li et al., 2005; Kalnins et al., 2002; Santavirta et al., 1998; Fabiola et al., 2016). Unlike many biocompatible materials, SiC has been proven to be a unique choice of the electrode material without experiencing the growth of tissues when it is implanted in the body (Saddow et al., 2010; Kalnins et al., 2002; Santavirta et al., 1998).

While the crystalline structure of SiC is critical for its biocompatibility, to achieve high sensitivity, electrochemical glucose sensors need a porous structure to enhance the liquid interface with the electrode. In this regard, various forms of conducting polymers (CPs) have been used for making sensor electrodes.

Among them, poly(3,4-ethylenedioxythiophene): poly(styrene sulfonate) (PEDOT:PSS) thin-films have been studied widely, due to higher enzyme immobilization capability, good electrical conductivity, better processability, excellent electrochemical stability, reliability, and biocompatibility (Yang et al., 2014; Aleeva et al., 2018; Pal et al., 2016; Xiao et al., 2013; Benoudjit et al., 2018; Liu et al., 2018). In addition to the use of a conducting polymer material, the surface structure also contributes to the effective immobilization of the enzyme. Of particular interest for this work is the utilization of electrospun nanofibrous structures, which offer large surface area, high porosity, biocompatibility, and dimensionality advantages, leading to better binding of the enzyme with the electrode for efficient electron-transfer and higher sensitivity (Puttananjegowda et al., 2020a, 2020b; Seung et al., 2020).

* Corresponding author.
E-mail addresses: kavyashreep@usf.edu (K. Puttananjegowda), atakshi@usf.edu (A. Takshi), sylvia@usf.edu (S. Thomas).

https://doi.org/10.1016/j.bios.2021.113285
Received 19 March 2021; Received in revised form 17 April 2021; Accepted 18 April 2021
Available online 30 April 2021

In the present work, fabrication, morphological and electrochemical characterization of glucose oxidase (GO_x) enzyme entrapped in PEDOT: PSS CP with SiCNPs electrospun-nanofibrous-membrane (ENFM) based glucose sensing electrode were measured. In this novel structure, GO_x is the main element for the glucose detection, CP provides the porous structure for the electrode and SiCNPs was added to improve biocompatibility of the sensor for the future in-vivo and implantable devices. However as presented in this work, we have found that SiCNPs-ENFM exhibits higher sensitivity, better limit of detection and durability compared to the prior state-of-the-art glucose sensors (Aleeva et al., 2018; Pal et al., 2016; Xiao et al., 2013; Benoudjit et al., 2018; Liu et al., 2018; Puttananjegowda et al., 2020a, 2020b; Seung et al., 2020; Jedrzak et al., 2018; Ayenimo and Adeloju, 2017; Kumar, 2020; Singh et al., 2016; Vukojevic et al., 2018; Zaidi, 2016; Yun et al., 2011; Abd-Wahab et al., 2019; Chen et al., 2020; Saleem et al., 2021; Thomas et al., 2020). It has been shown that conducting polymers and SiCNPs could be utilized as mediator for detection of glucose. This is presumably due to direct electron transfer between GO_x and the CP, which is an oxygen-independent detection. This work is intended to study the feasibility of using SiCNPs-ENFM electrode for fabricating glucose sensors. The electrochemical behaviour of such electrode was studied for the detection of glucose. The results show the potential advantages of SiCNPs-ENFM electrodes for biosensors and measurement of glucose concentration.

2. Materials and experimental methods

2.1. Materials and apparatus required for the fabrication of glucose sensor

The PEDOT:PSS with 3.0–4.0% in H_2O, high-conductivity grade, D-Glucose with molecular weight 180.16 g/mol and potassium ferricyanide with molecular weight of 329.26 g/mol from Sigma Aldrich. The SiCNPs with molecular weight of 40.1 g/mol from Sigma Aldrich with the particle size of ~45–65 nm. The glucose oxidase from Aspergillus niger, tetrahydrofuran (THF), polyvinylidene fluoride (PVDF) with the molecular weight of ~534,000 was also from Sigma Aldrich were used for the fabrication of SiCNPs-ENFM electrode.

Following the recipe (Ruby et al., 2018), electrolyte solution was prepared using deionized water with 1:1 ratio of 5 mM potassium ferricyanide and 5 mM glucose. Sputtered chromium (100 nm) and gold (100 nm) on glass substrates were used for making working electrode (WE) and counter electrode (CE). Silver/silver chloride (Ag/AgCl) reference electrode (RE) was used in the electrochemical experiments.

2.2. Fabrication process of SiCNPs-ENFM glucose sensing electrode

The fabrication of an electrospun conducting polymer of PEDOT:PSS with addition of SiCNPs nanofiber based glucose sensor involves the following process steps; the solution for electrospinning was prepared by dissolving 1.18 g of polyvinylidene fluoride (PVDF) in 2 mL of tetrahydrofuran (THF), add 0.05 g of SiCNPs and add 0.22 g of PEDOT: PSS followed by vigorous stirring for 1 h at 60 °C. The resulting mixture was electrospun using the following parameters: single 18 gauge syringe nozzle; applied voltage of 20 kV; flow rate of 15 μL min^{-1}. The distance from the tip to the collector plate was fixed at 32 cm. A rotating mandrel was used to collect a bead free fibrous matrix, which helps the uniform distribution of fibers on the electrode surface. The gold coated glass substrate was affixed on to the mandrel surface and the mandrel was rotating at 54 RPM. After the fibers are spun on the gold surface of area 0.35 cm × 0.5 cm with the ENFM thickness of approximately 500 nm–600 nm, then the SiCNPs-ENFM electrode was dried at 70 °C for 4.5 h. The GO_x enzyme solution of 1.5 mg was drop casted over the nanofibrous membrane coated electrodes. For enzyme immobilization to occur, the electrodes were kept at less than 4 °C for 24 h. Fig. 1(a) illustrates the pictorial representation of the SiCNPs-ENFM electrode and Fig. 1(b) shows the photograph of the fabricated SiCNPs-ENFM glucose sensing electrode.

3. Results and discussion

3.1. Morphological characterization

The transmission electron microscopy (TEM, Tecnai TF20) were used to characterize the morphology of SiCNPs with 50 nm scale bar shows in Fig. 2 (a) and it's energy dispersive X-ray (EDX) spectrum graph is shown in Fig. 2 (b) has 1000 carbon, 2200 silicon and 50 oxygen indicates that the silicon and carbon is the significant elemental component in the nanoparticles. Scanning electron microscope (SEM, Hitachi SU800) were used to characterize the morphology of SiCNPs-ENFM. Fig. 2 (c) shows SEM micrographs with 25 kV acceleration voltage, 1100 magnification and 10 μm scale bar, of the fabricated conductive polymer based SiCNPs-ENFM without GO_x. These images depict a fibrous morphology structure having an average diameter range of 110–140 nm. Fig. 2 (d) shows SEM micrographs with 25 kV acceleration voltage, 1100 magnification and 10 μm scale bar, of SiCNPs-ENFM with GO_x of closely packed matrix like structures which facilitated higher GO_x surface coverage within the nanofibrous matrix. The larger surface area helped to promote the binding of the GO_x enzyme within the fibrous membrane of the electrode. As for the SiCNPs-ENFM electrode, when the sensor is placed in an electrolyte solution, the enzyme molecules binds with nanofibers which avoids the leaching out of enzyme molecules very fast, which affects the sensitivity, stability, repeatability and durability of the sensing electrode.

3.2. Electrochemical characterization

The cyclic voltammetry (CV), chronoamperometry (CA) and electrochemical impedance spectroscopy (EIS), were performed on VersaSTAT-4 by Princeton Applied Research (PAR), electrochemical

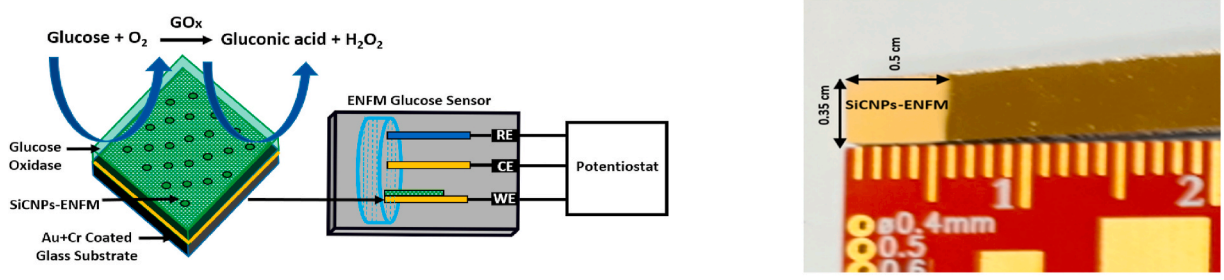

Fig. 1. (a) Pictorial representation of the SiCNPs-ENFM glucose sensing electrode (b) Photograph of the fabricated SiCNPs-ENFM glucose sensing electrode.

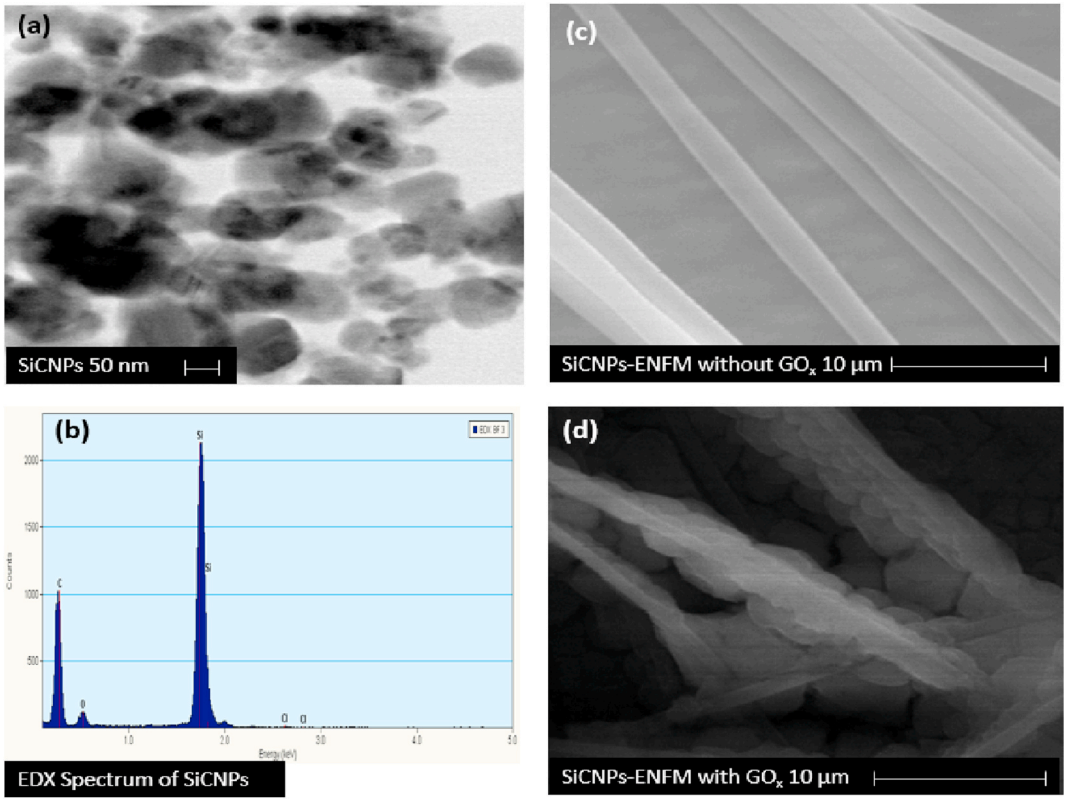

Fig. 2. (a) TEM image of SiCNPs (b) EDX spectrum of SiCNPs (c) SEM images of electrospuned PEDOT: PSS + SiCNPs nanofibers without GO_x (d) SEM image of electrospuned PEDOT: PSS + SiCNPs nanofibers with GO_x.

analyzer on a three-electrode system set up. The performance analysis of SiCNPs-ENFM Au/SiCNPs+PEDOT:PSS (nanofibers)/GO_x based glucose sensing electrodes were studied through electrochemical measurements such as CV, CA and EIS. The CV of SiCNPs-ENFM electrodes at 5 mM glucose concentration with a potential range of +0.9 V to −0.9 V at a scan rate of 75 mVs^{-1} were depicted in Fig. 3(a). The CV of SiCNPs-ENFM based electrode shows the oxidation peak of +1.52 mA around +0.6 V and reduction peak of −1.501 mA around −0.4 V. Despite the electroactivity of potassium ferrocyanide with the electrochemical potential of $E^0 = 0.156$ V verses Ag/AgCl (Bard and Faulkner, 2001), lack of any redox peak in that voltage range suggest negligible impact of potassium ferrocyanide in the glucose detection. Fig. 3(b) shows the CA graphs of the SiCNPs-ENFM electrode. At +0.6 V the maximum faradaic current was observed with a 5 mM potassium ferricyanide for glucose concentration ranges from 0.5 mM to 20 mM. The current response varies from 41.1 μA ± 0.0010 μA–146.2 μA ± 0.0013 μA for SiCNPs-ENFM electrode at the elapsed time of 60 s. From the calibration plots of Fig. 3(c), the sensitivity is calculated by slope (5.3828 μA/mM for SiCNPs-ENFM) divided by the surface area of the sensing electrode (0.35 cm × 0.5 cm) and the LOD (the lowest concentration that can be reliably detected) of the SiCNPs-ENFM electrode was found to be 30.75 μA/mM cm^2 and 0.56 μM. The EIS (Shervedani et al., 2009; Shervedani and Bagherzadeh, 2009) was performed for the SiCNPs-ENFM electrodes with equivalent circuit models at 5 mM glucose concentration with a frequency range of 0.1 Hz–10 kHz and an amplitude of 20 mV with the 0 V DC is represented in Nyquist plot which is shown in Fig. 3(d). The SiCNPs-ENFM based electrode exhibits the solution resistance (R_s) of 196.08 Ω and charge-transfer resistance (R_{WE}) of 28.58 Ω, double-layer capacitance (C_{WE}) of 2.78 μF and Warburg impedance of 418.16 $\Omega/\sqrt{s}$. The various electrochemical results from CV, CA, and EIS indicate that the SiCNPs-ENFM electrode shows the promising performance as glucose sensor. Durability of SiCNPs-ENFM electrodes were measured for 5 mM glucose concentration at +0.6 V potential and the electrodes were refrigerated at 4 °C. The CA measurements in Fig. 3(e), shows a lower change in current response for SiCNPs-ENFM based glucose sensing electrode was observed over 50 days period. Due to the porous structure of the compact nanofibrous matrix, GO_x enzyme molecules were entrapped on the nanofibrous membrane surface. These results are indicative of good durability through strong electrochemical responses when using SiCNPs-ENFM electrode, encouraging the application of nanofibers for the fabrication of potential biosensors in future. The great advantage of SiCNPs-ENFM verses solid SiC electrode is in its high flexibility suitable for in-situ detection of glucose benefiting the biocompatibility of silicon carbide.

From Table 1, it can be observed that the SiCNPs-ENFM glucose sensor has a significant improvement in performance showing better sensitivity, LOD, stability and durability, compared to the previously published state-of-the-art PEDOT conductive polymer based glucose sensors (Aleeva et al., 2018), (Xiao et al., 2013), (Puttananjegowda et al., 2020a), and (Chen et al., 2020).

4. Conclusion

Our results demonstrated the morphological and the electrochemical analysis of a SiCNPs-ENFM based enzymatic glucose sensing electrode which can be potentially used for monitoring the blood glucose level in diabetic patients for in-vivo measurements. Electrospun SiCNPs-CP nanofibers, used as a unique sensing electrode matrix improving the immobilization of GO_x. Hence a high sensitivity, low LOD with durability for up to 50 days was achieved. Further works are needed to test the biological interference study of the sensor to only glucose using real blood samples.

CRediT authorship contribution statement

Kavyashree Puttananjegowda: Conceptualization, Methodology,

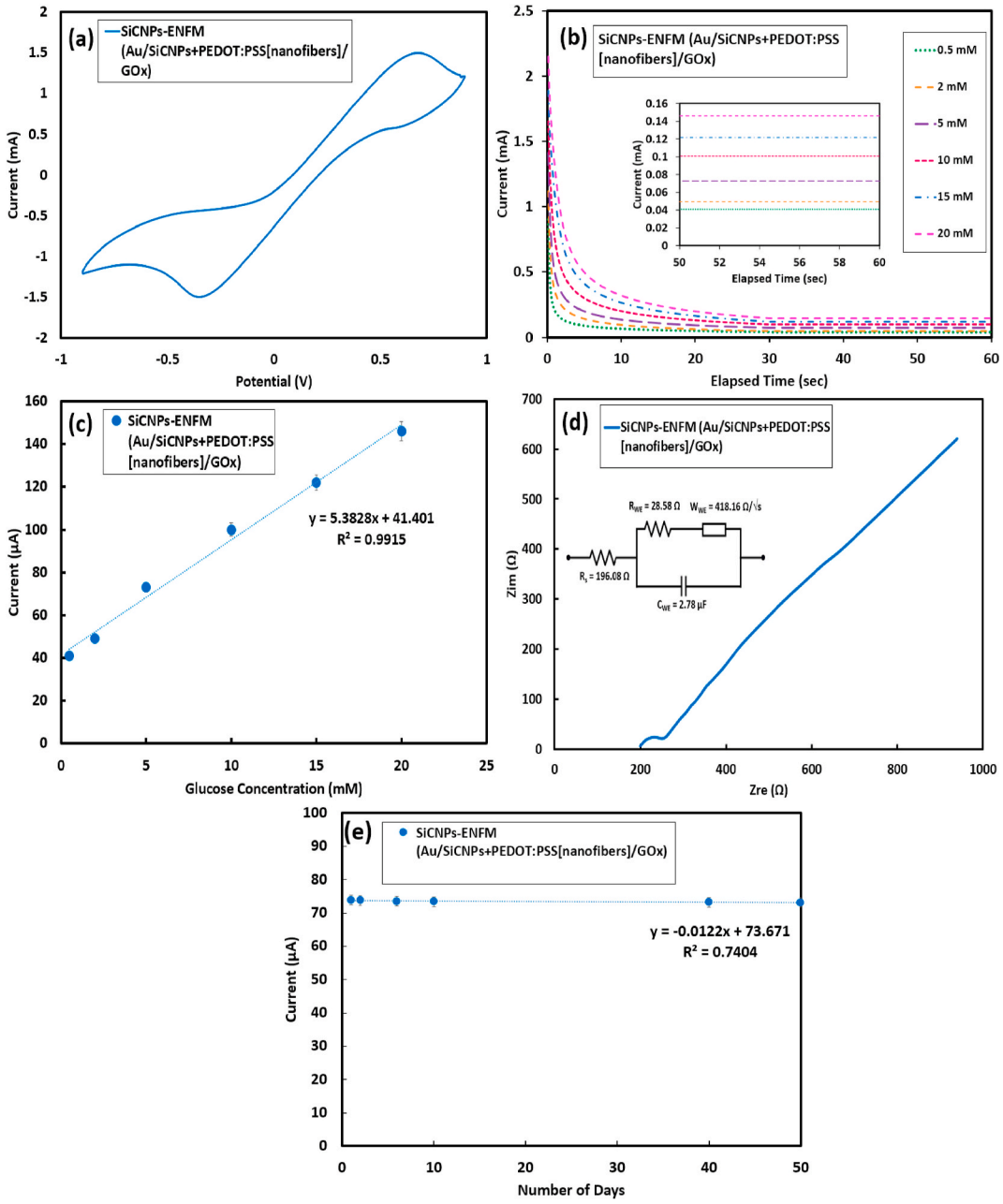

Fig. 3. (a) Cyclic voltammograms of SiCNPs-ENFM Au/SiCNPs-PEDOT:PSS (nanofibers)/GO_x electrodes at 5 mM glucose concentration with a potential range of +0.9 V to −0.9 V at a scan rates of 75 mVs^{-1}. (b) Chronoamperometric graphs of SiCNPs-ENFM Au/SiCNPs-PEDOT:PSS (nanofibers)/GO_x electrodes at potential +0.6 V. (c) Calibration plots of current response verses varied glucose concentrations (0.5 mM–20 mM) for SiCNPs-ENFM Au/SiCNPs-PEDOT:PSS (nanofibers)/GO_x electrode at an elapsed time of 60 s. (d) Nyquist plots of SiCNPs-ENFM Au/SiCNPs-PEDOT:PSS(nanofibers)/GO_x electrodes at 5 mM glucose concentration with an amplitude of 20 mV and the frequency range from 0.1 Hz to 10 kHz. (e) Durability of SiCNPs-ENFM electrodes and the error bars indicates the standard deviation of 6 experimental measurements.

Table 1
Comparison of SiCNPs-ENFM with PEDOT nanofibers based glucose sensors.

Reference	Aleeva et al. (2018)	Xiao et al. (2013)	Puttananjegowda et al. (2020a)	Chen et al. (2020)	This Work
Sensing Electrode	Pt/PEDOT-NFs/GO_x	NPG/PEDOT/GO_x	Au/PEDOT:PSS-PVDF-ENFM/GO_x	CF-PEDOT-NFs/GO_x	**Au/SiCNPs-PEDOT:PSS-PVDF-ENFM/GO_x**
Sensitivity	9.2 µA/mM cm^2	7.3 µA/mM cm^2	5.11 µA/mM cm^2	8.5 µA/mM cm^2	**30.75 µA/mM cm^2**
Limit of Detection	0.1mM	10 mM	2.3 µM	6.5 mM	**0.56 µM**
Concentration Range	0–10 mM	0.1–15 mM	0–25 mM	0.5–15 mM	**0.5–20 mM**
Number of Days	30 days	7 days	50 days	60 days	**50 days**

Data curation, Writing – original draft. **Arash Takshi:** Writing – review & editing. **Sylvia Thomas:** Supervision.

Declaration of competing interest

The authors declare that they have no known competing financial interests or personal relationships that could have appeared to influence the work reported in this paper.

Acknowledgment

The present research work was supported by a University of South Florida (USF) Graduate School Signature Doctoral Research Fellowship and the USF Nanotechnology Research and Education Center (NREC, www.nrec.usf.edu).

References

Ababneh, M.M., et al., 2017. IEEE Ubi. Comp. Elec. and Mob. Comm. Conf. 254–257.
Abd-Wahab, F., et al., 2019. Biosensors 9 (36), 1–15.
Aleeva, Y., et al., 2018. IEEE Sensor. J. 18 (12), 4869–4878.
American Diabetes Association, 2020. Diabetes Care 43, 5–8.
Ayenimo, J.G., Adeloju, S.B., 2017. Food Chem. 29, 127–135.
Bard, A.J., Faulkner, L.R., 2001. John Wiley & Sons Inc. 1–200.
Benoudjit, A., Bader, M.M., Wardatul, W., Salim, A.W., 2018. Sensing and Bio-sensing Research J. 17, 18–24.
Chen, J., et al., 2020. J. Electrochem. Soc. 167, 1–9.
Fabiola, A.C., Mumcu, G., Saddow, S.E., 2016. MRS Adva 1 (55), 3691–3696.
Gabriel, G., Erill, I., Caro, J., Gómez, R., Riera, D., Villa, R., Godignon, P., 2007. Microelectron. J. 38, 406–415.
Jedrzak, A., et al., 2018. Sensor. Actuator. B 256, 176–185.
Kalnins, U., Erglis, A., Dinne, I., Kumsars, I., Jegere, S., 2002. Med. Sci. Mon. Int. Med. J. Exp. Clin. Res. 2, 16–20.
Koschwanez, H.E., Reichert, W.M., 2007. Biomaterials 28 (25), 3687–3703.
Kumar, R., 2020. Nano-Micro Lett. 12 (122), 1–52.
Le, L.V., Chendke, G.S., Gamsey, S., 2019. J. Diabetes Sci. and Tech. 4 (2), 204–211.
Li, X., Wang, X., Bondokov, R., Morris, J., An, Y.H., Sudarshan, T.S., 2005. J. Biomed. Mater. Res. B Appl. Biomater. 72 (2), 353–361.
Liu, Y., et al., 2018. Biosens. Bioelectron. 100, 374–381.
Pal, R.K., et al., 2016. Biosens. Bioelectron. 81, 294–302.
Puttananjegowda, K., Thomas, S., 2017. IEEE Ubi. Comp. Elec. Mob. Comm. Conf. 16–19. https://ieeexplore.ieee.org/stamp/stamp.jsp?tp=&arnumber=8248971.
Puttananjegowda, K., Thomas, S., 2018. IEEE Info. Tech., Elec. and Mob. Comm. Conf. 383–388.
Puttananjegowda, K., Thomas, S., 2020. Analog Integr. Circuits Signal Process. 102, 659–666.
Puttananjegowda, K., Takshi, A., Thomas, S., 2020a. IEEE Sensors Lett 4 (2), 1–4.
Puttananjegowda, K., Takshi, A., Thomas, S., 2020b. J. Electrochem. Soc. 167 (3), 1–6.
Ruby, A., et al., 2018. Mater. Sci. Eng. C 90, 273–279.
Saddow, S.E., Coletti, C., Frewin, C.L., Schettini, N., Oliveros, A., Jarosezeski, M., 2010. Mater. Res. Soc. Symp. Proc. 12 (46), 193–198.
Saleem, K., et al., 2021. IEEE Sensor. J. 21 (4), 4167–4175.
Santavirta, S., Takagi, M., Nordsletten, L., Anttila, A., Lappalainen, R., Konttinen, Y.T., 1998. Arch. Orthop. Trauma Surg. 118 (2), 89–91.
Seung, H.B., et al., 2020. Mater. Sci. Eng. C 107, 1–8.
Shervedani, R.K., Bagherzadeh, M., 2009. Sensor. Actuator. B Chem. 139 (2), 657–664.
Shervedani, R.K., et al., 2009. J. Electroanal. Chem. 633 (1), 259–263.
Singh, P., et al., 2016. Nano-Micro Lett. 8 (3), 193–203.
Thomas, S., et al., 2020. Conductive polymers and metal oxide polymeric composites for nanostructures and nanodevices. In: Guarino, V., Focarete, M.L., Pisignano, D. (Eds.), Advances in Nanostructured Materials and Nanopatterning Technologies. Elsevier, pp. 243–271.
Vukojevic, V., et al., 2018. J. Electroanal. Chem. 823, 610–616.
Xiao, X., Wang, M., Li, H., Si, P., 2013. Talanta 116, 1054–1059.
Xu, Y., et al., 2019. Sensors 19, 1–22.
Yang, G., Kampstra, K.L., Abidian, M.R., 2014. Adv. Mater. 26, 4954–4960.
Yun, Y.H., et al., 2011. The Japan Soc. Ana. Chem. 27, 375–379.
Zaidi, S.A., 2016. Talanta 149, 30–42.